AKADÉMIAI KIADÓ

Fatigue damage analysis of pavements under autonomous truck tire passes

Mohammad Fahad* and Richard Nagy

Department of Transport Infrastructure and Water Resources Engineering, Faculty of Civil Engineering, Széchenyi István University, Győr, Hungary

Received: January 2, 2022 • Revised manuscript received: March 4, 2022 • Accepted: April 7, 2022
Published online: June 24, 2022

Pollack Periodica • An International Journal for Engineering and Information Sciences

17 (2022) 3, 59–64

DOI:
10.1556/606.2022.00588

ORIGINAL RESEARCH PAPER

ABSTRACT

Two different tire configurations consisting of a dual tire and a super single wide tire having different range and distribution of contact pressures have been analyzed. Along with the effect of speed on development of pavement damage at speeds of 5, 50 and 80 km h^{-1} under zero and uniform wander modes. Results show that at super slow speeds of 5 km h^{-1}, at dual wheel moving at zero wander mode, decrease in fatigue life of the pavement is 3.5 years, which is 1.45 times more than the dual wheel moving at uniform wander and 3.4 times more than wide tire moving at uniform wander mode. The difference between fatigue damage at different lateral wander modes is prominent at speeds greater than 50 km h^{-1}. A wide tire performs better than the dual wheel under zero wander configurations.

KEYWORDS

autonomous trucks, lateral wander, fatigue cracking, ABAQUS code

1. INTRODUCTION

The use of autonomous trucks on highways could affect transport infrastructure in a variety of different ways in terms of improving fuel efficiency and traffic safety. However, there are critical affects related to fatigue damage on pavement structure. It has been observed that autonomous trucks will be programmed to use the traffic lane without any lateral movement causing increased concentration of loads along the wheel path [1]. On the other hand, human driven trucks follow the normal distribution pattern along the transverse direction within the lane [2].

Fatigue damage is a major form of distress in flexible and rigid pavements [3]. Fatigue cracking occurs in the pavement as a result of cumulative traffic loading on the pavements [4–6]. Low temperature conditions accelarate the progression of fatigue in pavement. [5, 6]. Fatigue damage in asphalt pavements is highly dependent on variation in temperatures and corresponding stress strain levels [7–9]. Since the human driven trucks never utilize the complete width of the lane hence the repetition of concentrated loading along the narrow region of wheel path is increased. Hence, higher accumulation of loads along the same point can result in development of fatigue cracks hence prematurely failing the pavement structure. Moreover, fatigue cracking prevails at much faster rate in regions with lower pavement temperature in winter climatic conditions [8].

Gungor et al. [9] developed a flexible pavement design framework termed as Wander 2D for optimizing the lateral coverage by autonomous trucks within the lane. The recommended framework was applied on Mechanistic-Empirical Pavement Design Guideline (MEPDG). Research concluded with possibility of MEPDG to be used for determining lateral wander impacts of autonomous trucks. Noorvand et al. [2], studied the impacts of various lateral wander modes and traffic composition of human driven and autonomous trucks. Analysis was conducted on MEPDG software. Research concluded with minimum recommended percentage of Autonomous Trucks (ATs) to be 50% in the traffic mix under a uniform lateral wander mode.

*Corresponding author.
E-mail: fahadmohammad854@gmail.com

AKJournals

Hadian et al. [10] used 3D Finite Element (FE) model for investigation of fatigue cracking progression in synthetic asphalt pavements. Tensile strain was measured at the bottom most part of the pavement. Moreover, the friction in between successive pavement layers was adjusted to measure its effect on deformation and fatigue cracking. It was found that increasing the elastic modulus of material layers could reduce the tensile strain by a small margin and fatigue cracking was prevalent in stiffer Asphalt Concrete (AC) mixtures. Chen et al. [11] used the 2D FE model to assess the impacts of various lateral wander modes of autonomous trucks on rutting and fatigue cracking. For fatigue cracking determination, Palmgren-Miner linear damage hypothesis [11] was used.

2. RESEARCH METHODOLOGY

A pavement with a lane width of 3.5 m is considered for this study. Since the pavement and tire assemblies are symmetric, only half the lane width of 1.75 m is considered for analysis. Two tire types are used for exerting the load pressure on pavement since the distribution of loading under a tire is non-uniform [12]. A typical four layered asphalt concrete pavement consisting of a 20 cm thick asphalt concrete surface layer, 450 cm thick aggregate base course, a 20 cm thick aggregate sub-base course and subgrade layer is considered for fatigue analysis. Extended pavement properties are shown in Table 1. Figures 1 and 2 show the illustrations of a dual tire and a super single wide tire assembly respectively.

2.1. Wheel loading and configurations

A nominal tire pressure of 720 kPa generated by an axle load of 75.6 kN has been used. Tire types used are a super single wide base tire 455/55R22.5 developed by Michelin and a conventional dual tire G159A-11R22.5 developed by Goodyear. Using two tire types having different contact pressures and lateral dimensions would be beneficial in

Table 1. Material properties used in ABAQUS code

Layer type	Thickness (cm)	Elastic modulus (kPa)	Poisson's ratio
Asphalt	20	950,000	0.41
Base course	40	500,000	0.35
Sub-base course	20	350,000	0.35
Subgrade	–	60,000	0.40

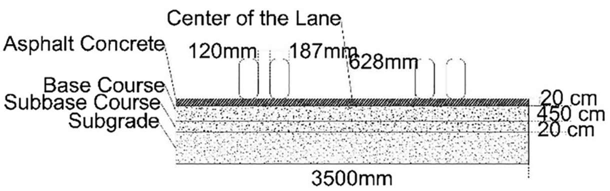

Fig. 1. Illustration of dual tire assembly on the pavement

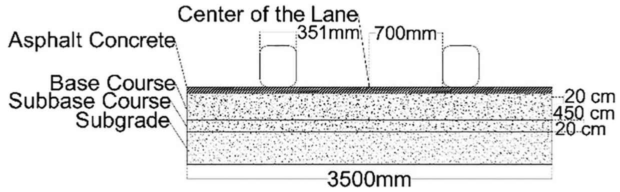

Fig. 2. Illustration of single wide tire on the pavement

analyzing the contact stresses at various wander modes and speeds as it is shown in Figs 3 and 4.

The footprint data has been taken from [12]. Since it has been proved that highest stress is exerted under the middle of tire [13] and the distribution of tire pressure under the tire is non-uniform [14–16], therefore, footprints for each tire configuration is shown in Figs 5 and 6.

2.2. Data preparation for ABAQUS code

Validated pavement material parameters have been taken from Cheng et al. [14] and are shown in Table 1. For vehicles weighing greater than 12 tons, three different speeds

Fig. 3. Digital tire footprint of a super single wide tire

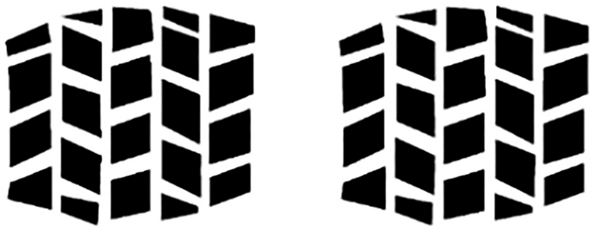

Fig. 4. Digital tire footprint of a dual tire

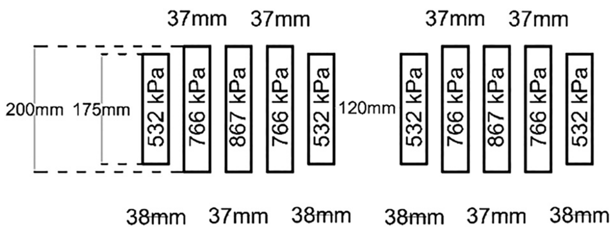

Fig. 5. Footprint details of a Goodyear G159A-11R22.5 dual tire used in simulations

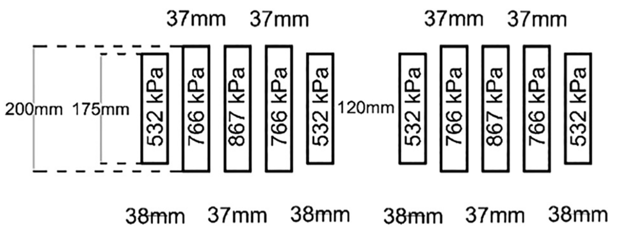

Fig. 6. Footprint details of a Michelin455/55r22.5 super single wide tire used in simulations

of 5, 50 and 80 km h^{-1} have been assumed and details of which are mentioned in Table 2.

Loading time used in ABAQUS code has been calculated by the method mentioned in [15], where based on the tire footprint size and the speed of simulated autonomous trucks of 5, 50 and 80 km h^{-1}, loading time was determined. Loading times for both zero wander and uniform wander modes were calculated for each step of loading. Zero wander modes consist two loading steps while the uniform wander mode consist of six total steps.

2.3. 3D FE model

A 3D model has been developed with longitudinal and lateral dimensions of 1.75 m by 1.75 m. Since a 2D model overestimates the damage progression in terms of vertical compressive strain on top of subgrade [14], hence a 3D model has been selected in this research. Moreover, dual and single tire assemblies are symmetric, hence half of the pavement width is considered for finite element analysis. The total depth of the model is 4.8 m, which includes all the pavement layers considered. Both the models have the same mesh density as well as element size to keep the results in maximum accuracy for the sake of comparison. Model element type is CPE8R. The model consists of total elements of 25,584 with an element size of 120 for increased accuracy as well as adequate calculation time. The 3D model has been designed to simulate the real-time pavement performance under loading; therefore layer to layer interaction property has also been added to the model. The developed 3D model has limitations in terms of added boundary conditions. Due to the complexity of the behavior of subgrade under loading, an elastic foundation under the bottom of pavement structure has been assumed. Figure 7 shows mesh formation of both models.

Table 2. Speed selection criteria

Speed	Scenario
5 km h^{-1}	Simulation of traffic congestion/ accident on highways
50 km h^{-1}	Speed limit for heavy goods vehicles on urban roads/passing through road works zones
80 km h^{-1}	Nominal speed of heavy goods vehicles in rural highways

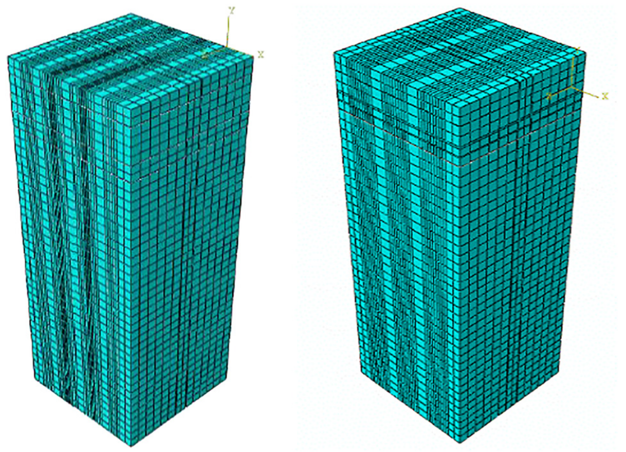

Fig. 7. Mesh details for dual tire (left) and single wide tire (right)

The interaction of layers in the pavement was kept as a normal surface-to-surface contact with hard and frictionless characteristics. For the boundary conditions, nodes were free to move along the normal directions but were restricted in perpendicular horizontal directions. The movement at the bottom of the model was restricted in all three directions. Figure 8 shows the loading and the boundary conditions for dual wheel and wide tire respectively.

3. RESULTS AND DISCUSSIONS

Simulation results from ABAQUS code have been presented for speeds of 50 km h^{-1} under zero wander and uniform wander mode for dual and wide tires combined. Simulations are conducted for a total of 30 million tire passes over a pavement design life of 15 years.

A noticeable contrast can be observed in the simulated strain values obtained for dual tire as compared to wide tire assembly as it is shown in Figs 9 and 10, clearly depict even distribution of load concentrations along the wheel path for

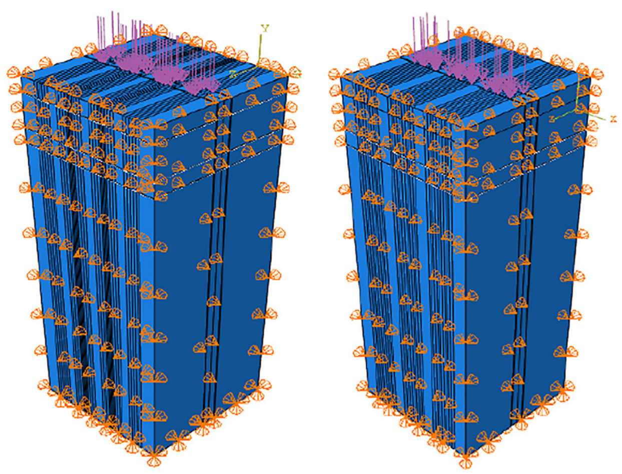

Fig. 8. Loading and boundary conditions for dual wheel model (left) and wide tire model (right)

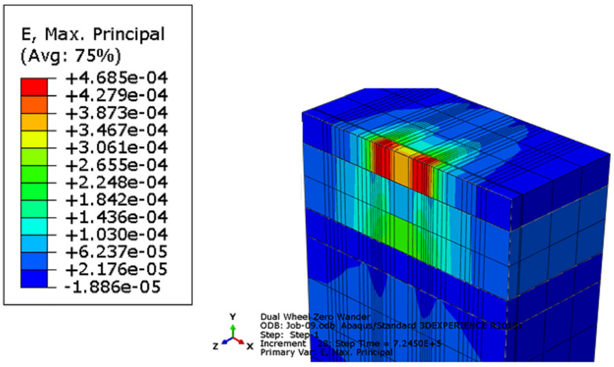

Fig. 9. Simulation results for 50 km h^{-1}, dual tire under zero wander mode

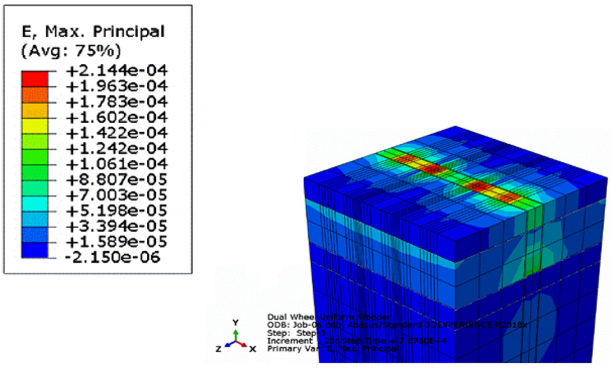

Fig. 10. Simulation results for 50 km h^{-1}, dual tire under uniform wander mode

a wide tire. Maximum strain values under the asphalt layer decrease by 45% when a uniform wander is used.

The highest strain value of 115 µm at speed of 5 km h^{-1} is obtained under the asphalt layer as it is shown in Fig. 11. The magnitude of strain values decrease mas the vehicles accelerated. However, it is noticed that the majority of peak strain values are concentrated in the center of the wheel path directly under each tire of a dual wheel assembly. Magnitude of accumulated micro-strains however decrease at a speed of

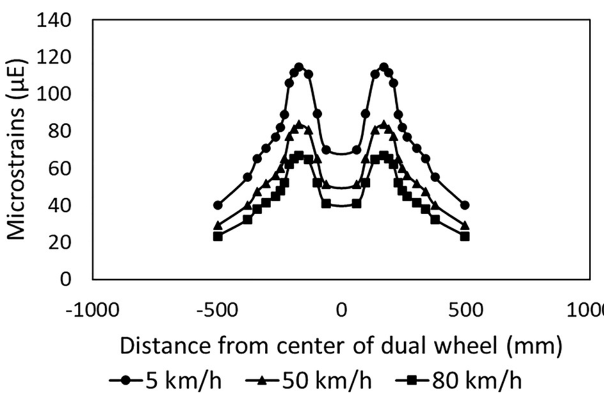

Fig. 11. Micro-strains measured at different speeds for dual wheel at zero wander mode

80 km h^{-1} with a value of 52 µm and however, in case of a dual wheel moving at uniform wander mode, as it can be observed from Fig. 12, the strain distribution is much even along the entire width of the lane and the magnitude is decreased by a factor of 25% at higher speeds.

Figure 13 shows only the resulting strains directly under the tire while Fig. 14 shows the resulting strains throughout the entire lane width. It can be observed that under a uniform wander mode, magnitude of strain values decrease by 30% when uniform distribution of loading is employed on

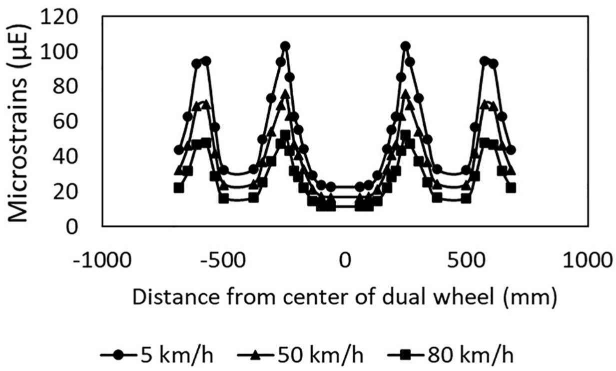

Fig. 12. Micro-strains measured at different speeds for dual wheel at uniform wander mode

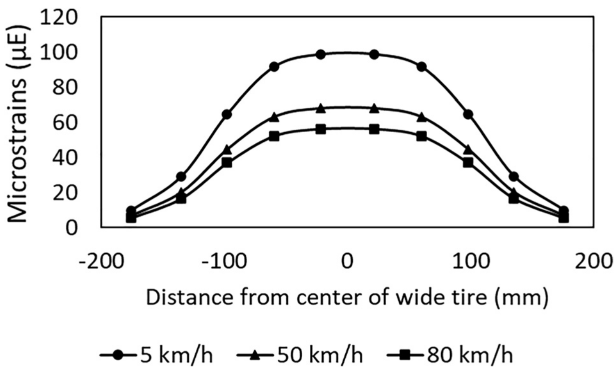

Fig. 13. Micro-strains measured at different speeds for wide tire at zero wander mode

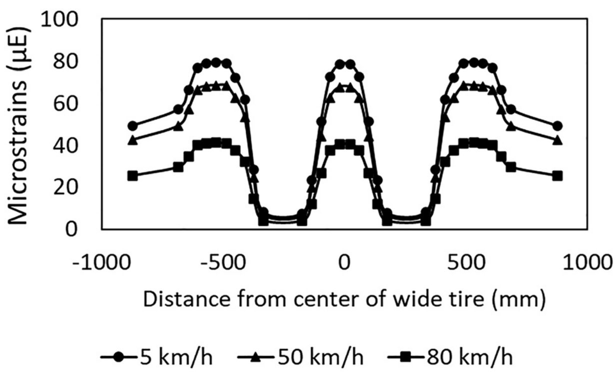

Fig. 14. Micro-strains measured at different speeds for wide tire at uniform wander mode

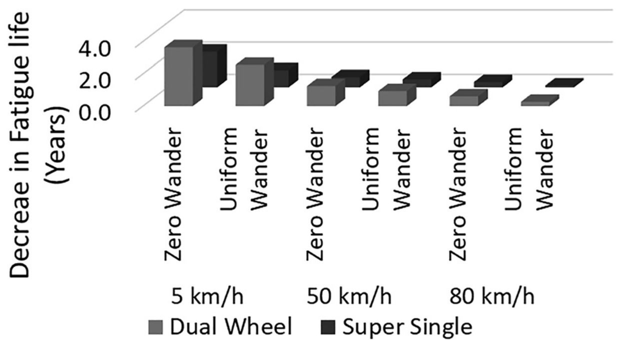

Fig. 15. Graphical representation of decrease in fatigue life under different speeds, tire configuration and lateral wander modes

the pavement. Uniform distribution of loading results in maximum micro-stain magnitude of only 41 μm as compared to 56 μm yielded by a tire moving under a zero wander mode at a speed of 80 km h^{-1}. The difference in micro-strains between zero wander and uniform wander is more pronounced at lower speeds as compared to dual tire assembly.

Palmgren-Miner linear damage hypothesis also termed as Miner's rule has been used in calculating fatigue damage and remaining number of tire passes for a specific period of time [13]. Fatigue characteristics are more prevalent during low temperature conditions [16] hence the tensile strain obtained under a specific location of the wheel path, the resulting fatigue damage can be calculated using the derived form of Eq. (1) [11],

$$D = \sum_{1}^{k} \frac{p_I n_I}{N_f(\varepsilon_i)}, \quad (1)$$

where p_I is frequency of loading, n_I is the accumulated axial loads, $N_f(\varepsilon_i)$ is the number of loads to reach fatigue life under strain ε_i and k is the number of lateral wander paths.

Thereby using Eq. (1), fatigue damage in number of reduced pavement lifetime was calculated and shown in Fig. 15.

Since the zero wander mode for both tire configurations cause concentrated loading cycles, therefor at normal operating speeds of 80 km h^{-1}, fatigue life decreases by a factor of 1.5 when a zero wander mode is used. The decrease in fatigue life is more pronounced at high speeds, specifically for a dual tire configuration. At super slow speeds of 5 km h^{-1}, fatigue life of a pavement can decrease by 3.5 years if zero wander modes is used. If a uniform wander mode is use at super slow speeds, still the minimum reduction in fatigue life stays at 2.6 years.

4. FINDINGS AND CONCLUSIONS

The key results in this study are mentioned below:

1. Strain decreases by a factor of 2.5 along the lateral distance away from the tire in case of dual wheel;
2. Strain decreases by a factor of 10 from the center of the wide tire to its edge for a dual wheel;
3. Increase in micro-strains is more prominent at lower speeds, since, micro-strains decrease by a factor of 0.5 while moving from 5 to 50 km h^{-1}, furthermore, micro-strains increase by factor of 0.3 while going from 50 to 80 km h^{-1};
4. In case of a dual wheel zero wander mode, decrease in micro-strains is more prominent at higher speeds since at lower speeds the load is still exposed to a specific point on pavement for a longer period of time;
5. Decrease in damage for dual wheel uniform wander mode is much less than that of a wide tire uniform wander mode because of wide lateral size of a dual tire assembly, due to which 60% of the wheel passes would always be concentrated in the center of the lane;
6. At super slow speeds, dual wheel moving at zero wander mode, decrease in fatigue life of the pavement is 3.5 years which is 1.45 times more than the dual wheel moving at uniform wander and 3.4 times more than wide tire moving at uniform wander mode;
7. When dual wheel uniform wander and wide tire zero wander is compared, the increase in fatigue damage for a wide tire zero wander is just 1.2 times more than that of dual wheel at uniform wander mode, hence even if high concentration of tire pressure is exerted, the uniform wander saves the pavement from increased fatigue damage.

It is recommended to employ the use of wide tire configurations along with uniform wander mode under recommended speeds of 80 km h^{-1} to limit severity of horizontal tensile strains acting under the asphalt layer in order to delay the occurrence of fatigue induced damage to pavements.

The current research has been limited to a specific type of asphalt pavement structure and loading mechanisms consisting of a conventional dual tire and wide tire assembly. This research does not take into account the effects of various driving axles of an autonomous truck. Moreover, the climatic conditions that would affect the properties of pavement structural layers and resulting in varied fatigue life have not been considered. For the future research, effects of various axles of a single autonomous truck shall be analyzed on the progression of rutting and fatigue cracking with various lateral wander modes.

REFERENCES

[1] F. Zhou, S. Hu, W. Xue, and G. W. Flintsch, "Optimizing the lateral wandering of automated vehicles to improve roadway safety and pavement life," *Transp. Res. Rec. J. Transp. Res. Board.*, vol. 2673, no. 11, pp. 37–43, 2019.

[2] H. Noorvand, G. Karnati, and B. S. Underwood, "Autonomous vehicles: Assessment of the implications of truck positioning on flexible pavement performance and design," *Transp. Res. Rec. J. Transp. Res. Board.*, vol. 2640, no. 1, pp. 21–28, 2017.

[3] Y. Zhefu, "Research on the fatigue damage of the asphalt pavement," *Appl. Mech. Mater.*, vols, 256–259, pp. 1776–1779, 2012.

[4] H. Di Benedetto, C. De La Roche, H. Baaj, A. Pronk, and R. Lundström, "Fatigue of bituminous mixtures," *Mater. Struct.*, vol. 37, pp. 202–216, 2004.

[5] F. M. Nejad, E. Aflaki, and M. A. Mohammadi, "Fatigue behavior of SMA and HMA mixtures," *Constr. Build. Mater.*, vol. 24, no. 7, pp. 1158–1165, 2010.

[6] K. Chatti, H. B. Kim, K. K. Yun, J. P. Mahoney, and C. L. Monismith, "Field investigation into effects of vehicle speed and tire pressure on asphalt concrete pavement strains," *Transp. Res. Rec. J. Transp. Res. Board.*, vol. 1539, no. 1, pp. 66–71, 1996.

[7] H. Cheng, L. Liu, and L. Sun, "Determination of layer modulus master curve for steel deck pavement using field-measured strain data," *Transp. Res. Rec. J. Transp. Res. Board.*, vol. 2673, no. 2, pp. 617–627, 2019.

[8] L. G. R. de Mello, M. M. de Farias, and K. E. Kaloush, "Effect of temperature on fatigue tests parameters for conventional and asphalt rubber mixes," *Road Mater. Pavement Des.*, vol. 19, no. 2, pp. 417–430, 2018.

[9] O. E. Gungor and I. L. Al-Qadi, "Wander 2D: a flexible pavement design framework for autonomous and connected trucks," *Int. J. Pavement Eng.*, vol. 23, no. 1, pp. 121–136, 2022.

[10] S. M. Hadian, "Investigation and analysis of fracture failure and fatigue cracking in high-rise pavement using simulation software of ABAQUS," *Ann. Civ. Environ. Eng.*, vol. 3, no. 1, pp. 032–039, 2019.

[11] F. Chen, M. Song, X. Ma, and X. Zhu, "Assess the impacts of different autonomous trucks' lateral control modes on asphalt pavement performance," *Transp. Res. Part C, Emerg. Technol.*, vol. 103, pp. 17–29, 2019.

[12] I. L. Al-Qadi, P. J. Yoo, M. A. Elseifi, I. Janajreh, G. Chehab, and A. Collop, "Effects of tire configurations on pavement damage," *Asph. Paving Technol. Assoc. Asph. Paving Technol. Proc. Tech. Sess.*, vol. 74, pp. 921–961, 2015.

[13] F. Wang and R. B. Machemehl, "Mechanistic-empirical study of effects of truck tire pressure on pavement: Measured tire-pavement contact stress data," *Transp. Res. Rec.*, no. 1947, pp. 136–145, 2006.

[14] H. Cheng, J. Liu, L. Sun, and L. Liu, "Critical position of fatigue damage within asphalt pavement considering temperature and strain distribution," *Int. J. Pavement Eng.*, vol. 22, no. 14, pp. 1773–1784, 2021.

[15] M. Fahad, R. Nagy, and P. Fuleki, "Creep model to determine rut development by autonomous truck axles on pavement," *Pollack Period.*, vol. 17, no. 1, pp. 66–71, 2022.

[16] T. Olexa and J. Mandula, "Comparison of complex modulus and elasticity modulus of bitumen bonded materials," *Pollack Period.*, vol. 11, no. 3, pp. 131–140, 2016.